Materials Science and Engineering C 29 (2009) 1266–1272

Contents lists available at ScienceDirect

Materials Science and Engineering C

journal homepage: www.elsevier.com/locate/msec

Repeat sequence proteins as matrices for nanocomposites

Lawrence F. Drummy [a,b,*], Hilmar Koerner [a,c], David M. Phillips [a,c], Joseph C. McAuliffe [d], Manoj Kumar [d,1], B.L. Farmer [a], Richard A. Vaia [a], Rajesh R. Naik [a,*]

[a] Materials and Manufacturing Directorate, Air Force Research Laboratory, Wright-Patterson AFB, OH, USA
[b] UES Inc., Dayton, OH, USA
[c] Universal Technology Corporation, Dayton, OH, USA
[d] Biomaterials Group, Genencor International Inc., Palo Alto, CA, USA

ARTICLE INFO

Article history:
Received 23 May 2008
Received in revised form 31 July 2008
Accepted 5 October 2008
Available online 18 October 2008

Keywords:
Silk
Elastin
Clay
Composites
Biomaterials

ABSTRACT

Recombinant protein–inorganic nanocomposites comprised of exfoliated Na^+ montmorillonite (MMT) in a recombinant protein matrix based on silk-like and elastin-like amino acid motifs (silk elastin-like protein (SELP)) were formed via a solution blending process. Charged residues along the protein backbone are shown to dominate long-range interactions, whereas the SELP repeat sequence leads to local protein/MMT compatibility. Up to a 50% increase in room temperature modulus and a comparable decrease in high temperature coefficient of thermal expansion occur for cast films containing 2–10 wt.% MMT.

1. Introduction

Proteins make up the main structural elements of most organisms, using complex sequences of amino acids that lead to wide arrays of functionalities. One of the most intensely studied structural proteins, *Bombyx mori* silkworm silk, has generated significant interest because of its remarkable mechanical properties, which rival even spider silk [1]. Elastin, another well-known structural protein, is found predominantly in the body's arterial walls, the lungs, intestines, and skin. Silk elastin like protein (SELP) is a recombinant protein consisting of alternating blocks of silk-like and elastin-like amino acid sequence domains that has been evaluated as a matrix for the controlled delivery of drugs, proteins, DNA and adenoviral particles [2–5]. While recombinant proteins like SELP are also of interest for in vivo structural applications such as tissue scaffolds [6], their mechanical properties are often inferior to structural proteins found in nature. Furthermore, the use of proteins in other applications both within and outside of the body requires enhancements of a wide variety of properties, including mechanical behavior in extreme environments including elevated temperature and loading conditions. As an example of nanocomposites for in-vivo applications, Barron and co-workers have explored the utility of aluminoxanes as reinforcement to poly(propylene fumarate)-bone tissue scaffolds [7].

In many cases in nature, proteins and peptides interact with inorganic materials, forming natural composite materials, such as in bones, seashells or diatoms [8–11]. These materials are formed by the self-assembly of proteins into various architectures which are then used as a template for inorganic materials to form. Here we use an alternative approach, similar to the approaches exploited to great success in the filled polymer industry. Rather than forming the inorganic component on the protein template, specific protein–inorganic intermolecular interactions are utilized to provide compatibility between, and uniform dispersion of, inorganic nanoparticles in the protein matrix. Although processed differently, the resulting nanocomposite structures mimic natural composite structures, like bone, in that the reinforcing inorganic phase is dispersed on the nanometer length scale.

Layered aluminosilicates [12], such as montmorillonite (MMT), have been successfully used as a nanoscale reinforcing phase for a wide range of commodity and experimental polymers [13,14]. Conceptually, fabrication methodologies pivot on the establishment of strong intermolecular interactions (electrostatic, dipolar or hydrogen bonding) between the polymer and MMT. MMT layers (1 nm thick, 30–300 nm diameter) are anionic and compatibility is nominally achieved through cationic surfactants, copolymers with cationic or hydrogen-bonding monomers, or polyelectrolytes, where surfactants are by far the most common. Researchers have investigated the formation of MMT nanocomposites based on synthetic

* Corresponding authors. UES Inc., Dayton, OH, USA.
E-mail addresses: lawrence.drummy@wpafb.af.mil (L.F. Drummy), rajesh.naik@wpafb.af.mil (R.R. Naik).
[1] Present address: DSM Innovation Center, 34256 Tupelo St., Fremont, CA 94555, USA.

0928-4931/$ – see front matter © 2008 Elsevier B.V. All rights reserved.
doi:10.1016/j.msec.2008.10.014

polyelectrolytes [15,16], water soluble hyperbranched polymers [17], polysaccharides [18], proteins [19,20], and polypeptides [21]. Several cationic polymers, such as polyamines [22], polyacrylamides [22], copolymers of acrylamide (AM) and trimethylaminoethylchloride acrylate (CMA) [23], and polyvinylpyridine [24] have been tested as intercalants or surfactants. However, only in some limited cases has the ability to controllably exfoliate the MMT in the matrix been demonstrated. For example, Denoyel et al. [23]. varied the polymer cationicity using AM/CMA copolymers and found that the maximum amount of polymer adsorbed onto the MMT particles at a polymer cationicity of 1%. Polymers with higher cation content evidently formed less loops and tails, rapidly attaching to the MMT surface and blocking further adsorption. Early polymer/layered silicate nanocomposites were produced using nylon as the matrix material, taking advantage of the ability of the polymer backbone to hydrogen bond [25,26]. Blends of hydrogen-bonding maleic anhydride-modified polypropylene with neat polypropylene are often used to improve intercalation of the polymer chains into the inter-layer galleries. Typically, only 0.1–0.2 wt.% maleic anhydride is needed to provide good dispersion of the layered silicate sheets in the matrix [27,28]. These results seem to be generally reflected in other studies implying that the optimal polymer–inorganic interfacial structure requires a balance between entanglements with the polymer matrix afforded by loops and tails, and a favorable interfacial energy afforded by 0.1–1 mol% of 'strongly' interacting co-monomers.

Proteins can have multiple functionalities in addition to localized charges, and in the case of SELP, several of these functionalities, such as moderate positive charge and the ability to hydrogen bond, can be exploited to produce well-dispersed nanocomposites. In this work we examine the effects of these functionalities on nanoparticle dispersion by comparing two recombinant proteins having the same repeat sequence of amino acids but with differently charged residues periodically occurring along the protein chain. When cast from solution, the MMT plates were extremely well dispersed, both on the local nanoscale and global microscale, within the SELP, even at volume fractions of greater than 10%. These resulted in improved room temperature elastic modulus and elevated temperature coefficient of thermal expansion for MMT concentrations up to 4–6%. When the SELP's positively charged lysine residues were replaced with negatively charged functional groups, the dispersion of MMT on the nanometer length scale remained excellent, however the uniformity of mixing on the micron length scale was diminished.

2. Results and discussion

Nanocomposites were formed via solution blending of MMT and SELP in de-ionized water, with Fig. 1A showing an optical picture of the resulting films (2% and 10% MMT loading), which demonstrated excellent optical clarity. X-ray scattering in the small and wide angle regimes of the dried SELP nanocomposite films are summarized in Fig. 1B. As the film casting process induced significant alignment of the MMT sheets parallel to the film surface, mounting films with the surface nearly parallel to the incident beam is necessary to maximize potential (00l) interlayer scattering in transmission geometry [29,30]. Neat MMT powder (at relative humidity ~50%, data not shown) exhibits an interlayer spacing near $q = 0.83\ \mathrm{nm}^{-1}$ (1.2 nm) and the (020) and (110) internal lattice reflections at $q = 2.2\ \mathrm{nm}^{-1}$ (0.45 nm). SELP exhibits 3 broad peaks at approximately $q = 0.23$, 1.0 and 2.2 nm^{-1}. SELP does not form crystalline secondary and tertiary structures in films with or without MMT as evidenced by the absence of the characteristic silk I peak at $d = 0.72$ nm [31] as well as the lack of any clear silk II β-sheet peaks [32]. The 0.72 nm peak has been seen in SELPs with high silk (GAGAGS) ratios [33,34], and it is likely that the high amount of non-crystallizable elastin inhibits any crystallization of the short silk segments in this case. Circular dichroism from SELP in aqueous solution (data not shown) gives a random-coil plus helical conformation, and more detailed studies to detect any conformational changes on the SELP on the MMT surface are currently underway. For the nanocomposites, no scattering from interlayer correlation is seen for systems with <6 wt.% MMT, where as a weak broad reflection ($0.07 < q < 0.4\ \mathrm{nm}^{-1}$) begins to develop at the highest MMT loading (10 wt.%). The MMT concentration in these nanocomposites is sufficient to provide interlayer scattering if significant interlayer correlations were present, since the intralayer (020) and (110) reflections are clearly observable. The broad SELP reflections at $q = 0.23$ and 1.0 nm^{-1} are observed at the lower MMT concentrations but are less distinguished at higher concentrations, potentially implying that the dispersed MMT impacts the microphase separation of the SELP. The small angle regime ($q < 1\ \mathrm{nm}^{-1}$) exhibits a uniform scattering profile indicating the absence of a well-defined intermediate or intercalated structure. The scattering intensity scales as $q^{-2.1}$ which is close to the expected scaling of q^{-2} for scattering from disks [35].

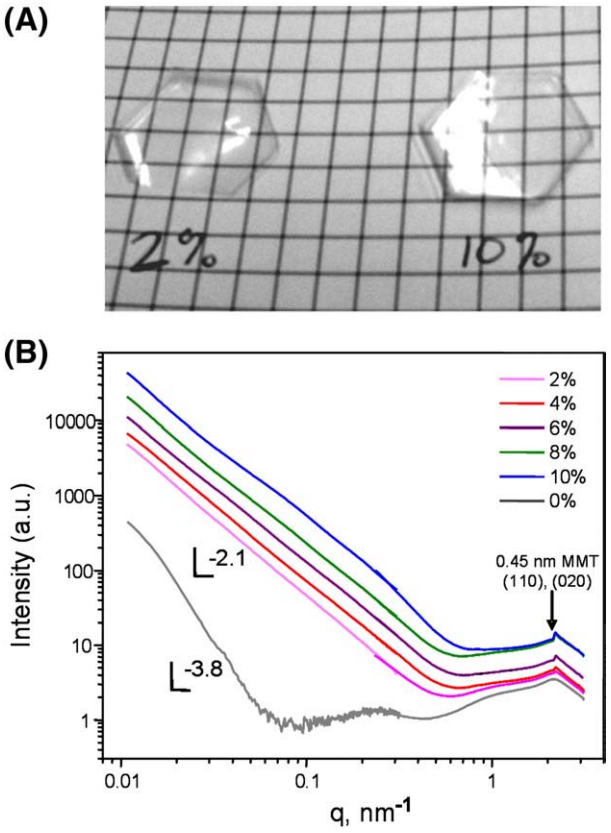

Fig. 1. (A) Optical image of the MMT/SELP samples with 2% and 10% MMT loading. X-ray scattering curves for the MMT/SELP samples. The curves show a log–log slope of −2.1 in the small-angle regime. The wide-angle regime clearly shows some scattering from the amorphous SELP and the peak at 0.45 nm from the (110) and (200) planes of the MMT lattice. No inter-layer peak from the MMT sheets is seen, indicating exfoliation.

Transmission electron micrographs from 150 nm thick cross-sections of 2%, 4% and 8% MMT in SELP nanocomposite samples are shown in Fig. 2. The high magnification micrographs (2b, d, f) show that the MMT is dispersed extremely well in the SELP matrix, with the individual, 1 nm thick, MMT sheets clearly visible. The density of MMT also appears to be quite uniform across the films from top to bottom, and along their length for several hundreds of microns (Fig. 2A, C, E). Alignment of the sheets could be seen near a film edge, and also throughout the films, with the sheets lying parallel to the film surface. This alignment is expected to occur during the slow drying process. Overall, the X-ray scattering and TEM analysis are consistent, confirming not only local but global uniformity of dispersed 1 nm MMT sheets.